LA-UR-16-24652
Approved for public release; distribution is unlimited.

Title: A 1-D Study of the Ignition Space for Magnetic Indirect (X-ray) Drive Targets

Author(s): Cobble, James Allen
Sinars, Daniel Brian

Intended for: A white paper for NNSA

Issued: 2016-07-06

A 1-D Study of the Ignition Space for Magnetic Indirect (X-ray) Drive Targets

June 2, 2016

J. A. Cobble
Los Alamos National Laboratory

D. B. Sinars
Sandia National Laboratories

Executive Summary

The ICF program today is investigating three approaches to achieving multi-MJ fusion yields and ignition: (1) laser indirect (x-ray) drive on the National Ignition Facility (NIF), (2) laser direct drive (primarily on the Omega laser facility at the University of Rochester), and (3) magnetic direct drive on the Z pulsed power facility. In this white paper we briefly consider a fourth approach, magnetic indirect drive, in which pulsed-power-driven x-ray sources are used in place of laser driven sources. We first look at some of the x-ray sources studied on Z prior to 2007 before the pulsed power ICF program shifted to magnetic direct drive. We then show results from a series of 1D Helios calculations of double-shell capsules that suggest that these sources, scaled to higher temperatures, could be a promising path to achieving multi-MJ fusion yields and ignition. We advocate here that more detailed design calculations with widely accepted 2D/3D ICF codes should be conducted for a better assessment of the prospects.

Magnetic X-ray Drive Platforms

There are two or more, incompletely explored x-ray-drive hohlraum designs available at Z. The first is the so-called dynamic hohlraum (DH). From the abstract of Ref. 1, "The Z-pinch dynamic hohlraum is a high-power x-ray source that has been used in a variety of high energy-density experiments including inertial confinement fusion (ICF) studies. The system consists of a tungsten wire array Z pinch that implodes onto a low-density CH_2 foam converter launching a radiating shock that heats the hohlraum to radiation temperatures >200 eV". The authors go on to share that Z could deliver 1.8 MJ of energy in a pulse that lasts as long as 10 ns. While this drive has its difficulties, Sanford[2] has published the peak temperature of the shock front in a dynamic hohlraum. In Fig 1, this has been modeled as a Gaussian curve with peak radiation temperature T_{rad} of 274 eV and an e-folding time of 5 ns. While this drive has its difficulties, the thought[3] was that "one can envision a more optimistic scenario in which it might be discovered that the radiation field directly inside of the central cylinder is very uniform. If this were to be the case, one might find that a capsule could absorb significantly more x-ray energy with a higher peak intensity if the capsule were placed directly in the center of the central cylinder… In this situation, the imploding cylindrical shell of tungsten plasma would be, in effect, a dynamic hohlraum wall" as is pictured in Fig. 2. This optimistic concept was mainly studied on Z prior to its refurbishment in 2006. Since 2007, the current delivered to these dynamic hohlraum targets has been increased from 22 MA to 26 MA as part of the development of this platform as a source for opacity experiments, but the platform has not been used for ICF experiments. While we must say that the asymmetries of this drive are extreme, that

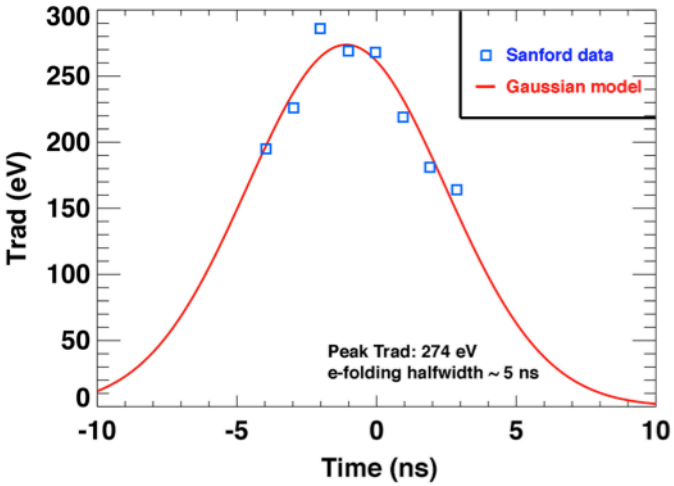

Figure 1. Best-fit Gaussian fit for the radiation temperature of dynamic hohlraum data of Ref. 2.

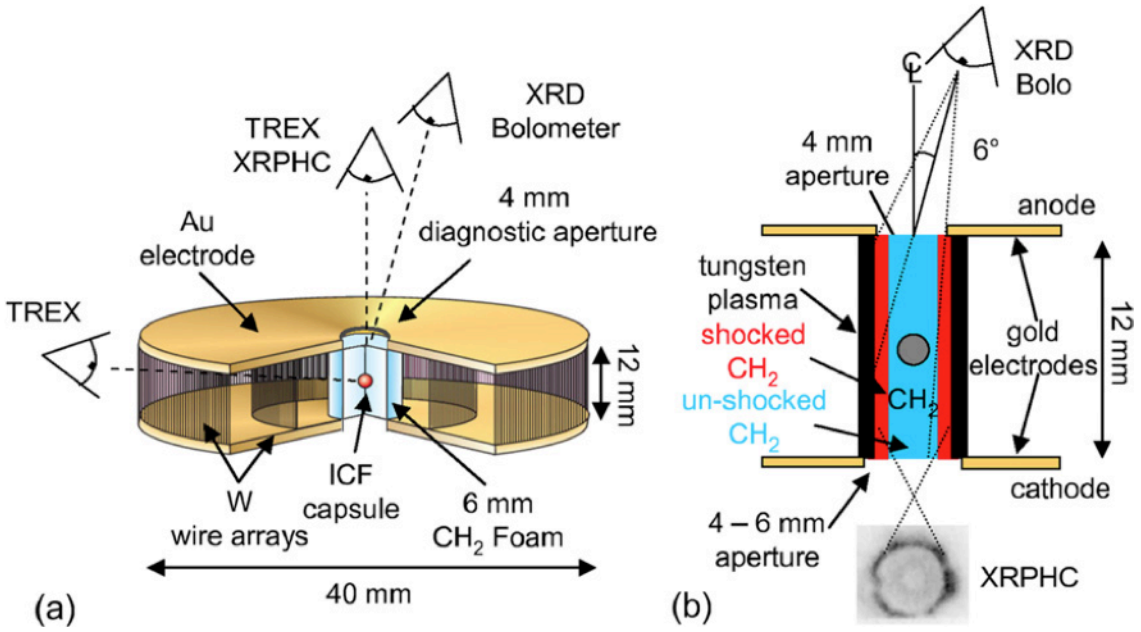

Figure 2. (a) Sketch of a Z-pinch dynamic hohlraum and (b) a magnified schematic of it after the W wire array has collapsed onto the plastic converter. (Fig. 1 of Ref. 3)

gymnastics with shine shields to make it more symmetric are problematic, and that the radiation temperature in Fig. 1 is overly optimistic, the drive is hot, there is lots of it, and the authors[3] show a way to fix it. Clearly, a double-ended DH drive with ZR (Z refurbished) is more suitable[4] from a symmetry perspective because a hohlraum between two wire arrays would not be crushed equatorially. The hohlraum would look like a conventional NIF hohlraum with the '*laser entrance*' hole diameter commensurate with the diameter of the stagnated wire arrays. The conceptual picture of this geometry is seen in Fig. 3. Notably, this configuration could be electrically driven either in series or in parallel. We will not discuss series/parallel except to say that one of these might be superior for top-bottom symmetry and the eliminations of P_1 Legendre modes. Either of these might be a way to accomplish our goal with the DH concept – uniform drive.

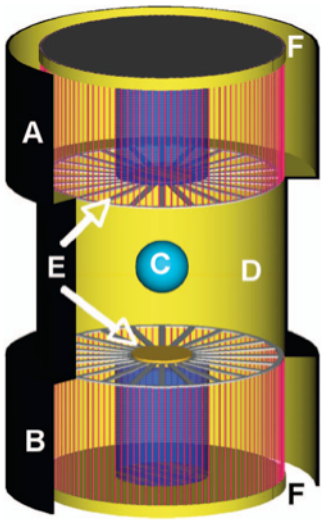

Figure 3. This image from Ref. 4 shows a possible double-sided hohlraum drive free from – not crushed by – the collinear wire arrays (A and B). The capsule (C) is centered in the secondary hohlraum (D) between the wire arrays. The spoke-like structures, return-current paths, attach to permanent shine shields (E) to protect the capsule from direct radiation and as secondary-cavity 'end caps' to limit loss along the axis from that volume. The electric power feeds are on the top and bottom (F).

An example of how shine shields might be used to divert radiation into a double-ended hohlraum is suggested in Fig. 4. This concept was demonstrated[5] with a sub-mm halfraum – half of a two-sided Au hohlraum – illuminated with two beams of the Trident Laser at Los Alamos National Laboratory, similar to the British Helen halfraums. The conical Au shine shield was mounted on a plastic webbing captured between the telescoping sleeves of the cylindrical portion of the hohlraum wall. With less than 300 J of Trident laser drive, we measured $T_{rad} \sim 140$ eV with an axial x-ray diode array behind the cone. The absence of the 'spoke array', *E* in Fig. 3, is not an issue on Z, as pointed out by Hammer[6], because the Be spokes are transparent to the x-ray drive. On an upgraded Z, the hohlraum would be optimized to provide the highest possible symmetric drive to the fuel capsule. Cuneo[7] discusses the symmetry issues associated with 20-MA experiments on Z and finds that even-numbered Legendre modes have radiation symmetry at the 3% level with single-shell ICF capsules. Vesey in Table II of Ref. 4 states that a majority of Z shots are expected to satisfy P_1 symmetry requirements. And, Hammer, whose paper[6] describes generic hohlraum scalings, goes on to embrace the idea that the path to ignition could include pulsed-power-driven indirect drive. There are alternative ways to create more efficient double-ended hohlraums on Z than alluded to by Hammer that we will not discuss in detail here.

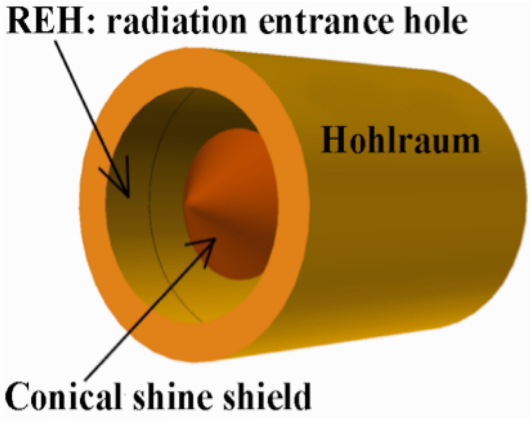

Figure 4. Modified hohlraum from Ref. 5. Symmetry is provided by a second source on the right side. The fine, black line denotes the edge of the plastic support web.

A unique feature of z-pinch-driven hohlraums is that there are no laser-plasma instabilities (LPI), and minimal x-ray preheat exists since high-energy bremsstrahlung from Z tends to come late in time. [Preheat is discussed in Appendix A.] The other good news is that radial diagnostic access is easier than with a single DH array, for example.

We already know from >6-ns laser hohlraums[8] that within 3 – 4 ns, the radiation flux inside becomes Planckian. Integrated wall radiation dominates laser "hot-spot" flux more and more later in time. The same equilibration will apply with x-ray drive since no multi-photon interactions are needed to make x rays, and there are neither hot spots nor LPI. Although the hohlraum must be modeled, the *ad hoc* assumption is that one or more of these Z platforms will provide uniform capsule drive and avoid the time-dependent Legendre modes that have been observed at NIF[9] and the equatorial crush[10] associated with dynamic hohlraums at Z.

Double shell design: We shall use the commercial 1D simulation code Helios[11] to model performance of double shell capsules. The code includes radiation and magneto-hydrodynamics with atomic-kinetics modeling. It is a useful resource to optimize shock timing and compression, derived from variations of shell (layer) properties. We are concentrating on the LANL[12] NIF point-design double shell shown in Fig. 5 on account of the inherent advantages associated[13] with their use. In the double-shell design, a low-Z

ablator, like Be-Cu, efficiently absorbs the hohlraum drive. It magnifies the energy density as it undergoes spherical convergence and transfers the pressure to the inner shell. The DT-filled inner shell, typically a Au-Cu mixture, compresses the gas – no DT-ice layer is required – and inhibits radiative losses from the gas as it heats. It also adds inertia and mass to delay fuel disassembly. One major difference from single-shell designs is that the double shell uses volume ignition – not central hot-spot ignition. Careful pulse shaping is less important. Ref. 13 cites additional advantages. Double shells have a lower peak implosion speed for ignition and relaxed symmetry requirements because of *i*) lower necessary convergence and *ii*) possible erasure of hydro instabilities. It has a lower ignition temperature (4 keV versus ~10 keV for central hot spot), and requirements for cryogenics may be relaxed. This latter advantage may not be fully realizable because many hundreds of atmospheres of gas at room temperature are needed for yield, and the means to do that may be lacking. Regardless, we have to mount the capsule in a vacuum hohlraum, and a fill tube could perform that task. Target-fab issues are beyond the scope of this paper.

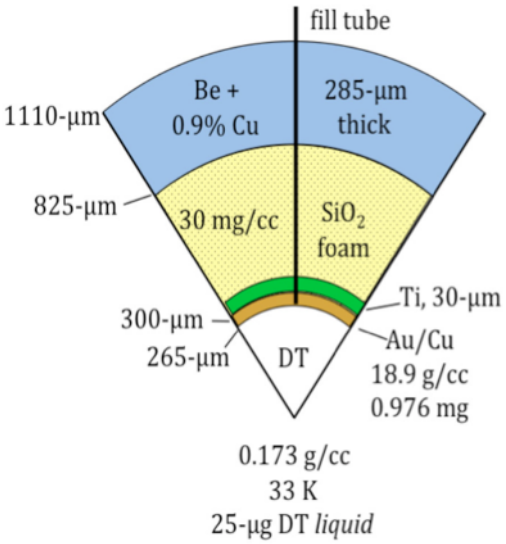

Figure 5. The LANL point-design for NIF double shell capsules

Though we are starting with the NIF point design, because the ZR drive is different, we shall alter the thicknesses of the two metal shells – one at a time – to optimize for shock coalescence and fusion yield. DT gas will be used in the Helios simulations because if we come close to ignition, alpha heating is a sensitive measure for optimization. Keeping in mind that a 3D simulation is more appropriate, this exercise could lead to cylindrical hohlraum x-ray drive that is relevant to similar physics issues common to the NIF platform – a benefit for the entire ICF enterprise. Were such experiments performed on ZR successfully, to state the obvious, it is recognized that upgrades for Z are both more feasibly and less expensive than upgrades on NIF. This too is beyond the scope of this paper; so, we next consider what the Helios simulations suggest.

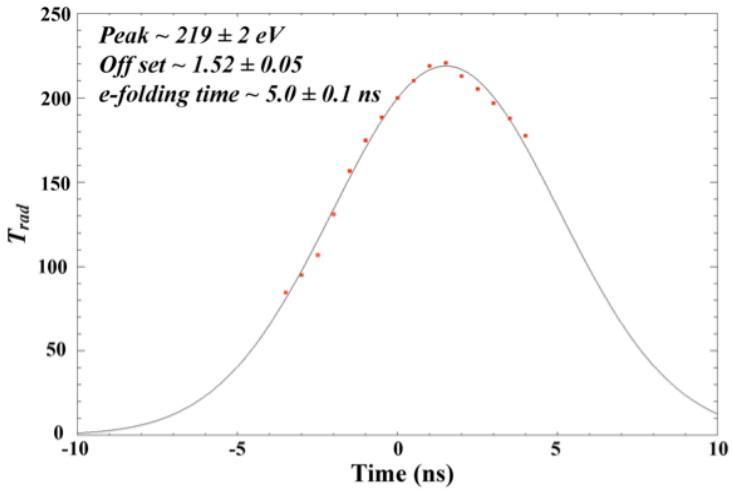

Figure 6. A symmetric radiation drive history that could be achievable at Z

The ZR T_{rad} Model: We use data recorded for T_{rad} for a high-current (~26

MA)[14] wire-array DH. It is from a slightly different geometry than the above description, but the total energy is in line with the above concept and the double-ended configuration avoids the asymmetries in a straight-forward way. Figure 6 shows the time history of the measured drive[14] with the least-squares best-fit parameters. For the 1D Helios model, we take necessarily the *ad hoc* position that this drive will be absolutely symmetric.

Simulations and results: The Helios simulations are based on this drive and the capsule illustrated in Fig. 5 with two exceptions. We used Be, not a Be-Cu (1%) ablator, and for the inner shell, we used a pure Au layer. The *ad hoc* assumption is that Cu represents an unnecessary heat sink for the ablator, as we shall see, and that for the Au layer, the Cu is not especially important. Table 1 shows the target layers and settings for the initial

Table 1. Initial Helios settings for the double-shell capsule

Region (Layer)	Thickness	Equation of State	Opacity	Outer Radius
DT 50%-50% by atom*	265 μm	DT.prp	DT.prp	265 μm
Au	35	matr_002700.ses	Au_DOELabDistrib_Dec2012.prp**	300
Ti buffer	30	Ti.prp	Ti.prp	330
30-mg/cc SiO2 foam	495	SiO2.prp	SiO2.prp	825
Be ablator	285	Be.prp	Be.prp	1110

* Region 1 pressure: 846 atm at STP; equivalent to 0 .173 g @ 33 K (liquid)
** According to the vendor, this is an averaged opacity, available only for the labs.

simulation. The results were modest; so, at the recommendation of David Montgomery, the capsule radius was made 10% larger to couple in more radiation drive (1D, uniform), and the mass in the outer Be shell was conserved. The foam layer mass was not conserved but at 30 mg/cc, this is not necessary. LANL target fab, by the way, can produce foam densities[15] from 20 – 200 mg/cc ± 2%. With the enhanced surface area, the yields became impressive. Notably, alpha-heating was 'turned off' in Helios because of the benefit of fast run times – not having to calculate ion transport. The optimization of DT-neutron yield versus layer thickness is shown in Fig. 7. Comparison to simulations with 1% Cu in the Be shell resulted in a factor or 4 – 6 decrease in yield *with the preheat shield* – demonstrating that Cu is a heat sink. For the

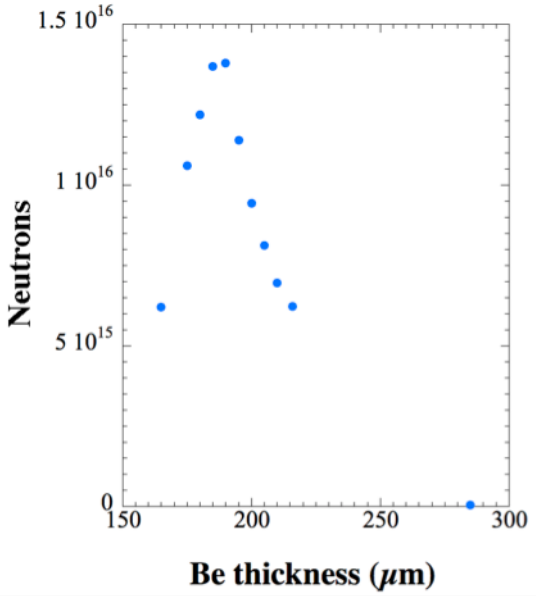

Figure 7. DT-neutron yield without alpha heating from Helios simulations of the enlarged capsule (1221 μm radius)

optimum case, a Be ablator of 190 µm, *alpha heating* was turned on with a resulting 1D yield of 1.2 x 10^{18} neutrons – 2.7 MJ. The NIF-point design case with a 285-µm Be-Cu ablator is shown to the right in Fig. 7.

Helios calculated the maximum DT mass density at the interface with the inner Au-layer wall, from which the compression ratio (CR) could be calculated. The density dependence on Be-ablator thickness is seen in Fig. 8. For all the cases near the peak, the CR was 10 – 10.6. The ion temperatures, while more scattered, were $T_i = 3.4 \pm 0.3$ keV. For the *alpha-on* case, T_i rose to >8 keV! This result speaks for itself.

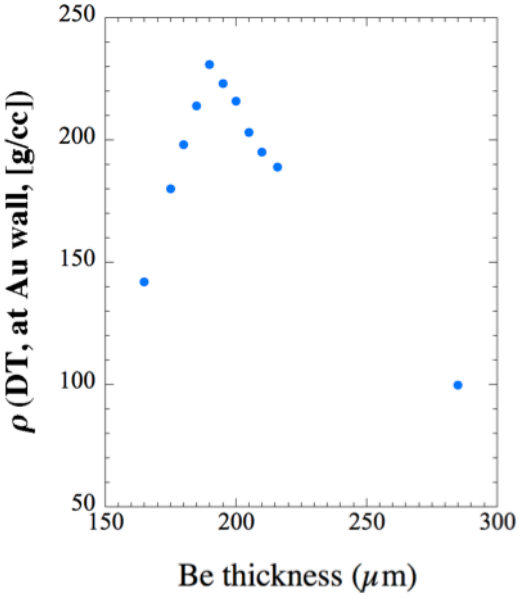

Figure 8. DT mass versus Be thickness

Because Helios is 1D, mix is absent from the calculations. Thus, for illustrative purposes, we used a common assessment to estimate how mix may degrade yield. In Figure 9, we show a fall-line analysis with the assumption that consistent with the intercept of the fall line at zero radius, mix quenches yield. From the Helios simulation of time-dependent burn (without alpha heating), at the indicated fall-line intercept, the yield is 6 x 10^{15} neutrons. The peak burn rate occurred at 12.86 ns.

Thus the loss estimate is about half the yield. This loss is not a particular concern because theoretically, one can also increase the drive to have robust burn, and this will be the conclusion of the white paper. As an aside, the figure incidentally shows that 30 or more of the initial 100 zones in the Be ablator are still present at bang time.

Besides neutron yield, Helios maps of plasma fluid velocity for different zones in the simulation were used to assess the quality of implosions and the coalescence of shocks in the core. Disturbing bumps and wiggles in the traces could indicate an incorrectly timed shock history. We see in Fig. 10, the velocity history of the optimum case with alpha heating turned off. Three zones are plotted. Zone 110 is the central zone in the Au shell. It is the first zone of the three plotted zones that sees the shock, indicated by the negative velocity. The next zone

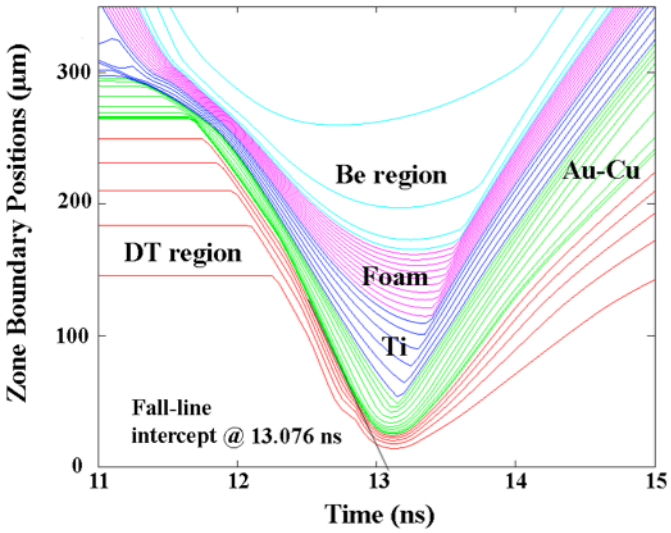

Figure 9. Fall-line analysis of the optimum case, alpha heating 'off' – The different colors indicate the five different layers in the Helios calculation. Every tenth zone boundary in the 1D calculation is illustrated.

that is shown is Zone 61, the inner-most Au zone – the only Au zone in contact with DT gas in 1D. It has a very similar velocity history. Zone 30 is the central zone (of 60) in the gas. It has a persistent spike in its velocity history that occurs before the fall line intercept and the minimum radius at 13.2 ns. Consequently, it has nothing to do with fusion (or mix in 1D). The gas zones throughout this phase of the implosion are still directed inward as long as their velocity is negative. What's more important, it is the absence of early-time features on this plot that shows the quality. No shocks are breaking out into the gas before 11.5 ns.

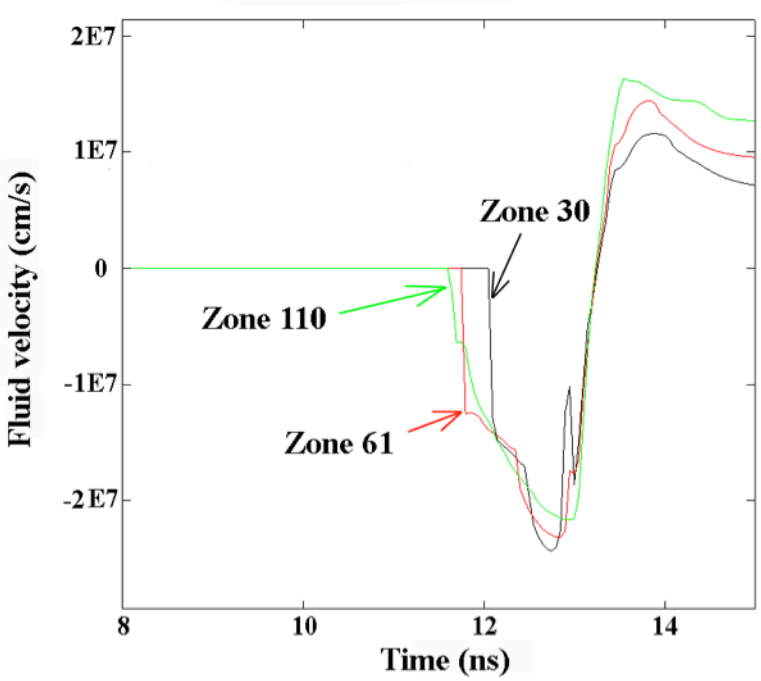

Figure 10. Implosion velocities of various zones in the simulation – Zone 110 is the central Au zone; 61 is the inner-most Au zone; 30 is the central DT zone.

Another thickness scan was performed, following this first optimization, on the thickness of the Au shell. To hold the capsule radius constant, we thinned this layer on the inside, incrementally increasing the DT layer radius in the process. Because the pressure in the DT region is held constant, this results in an increase in the volume of DT in these later simulations, but we can normalize yield by DT volume. The results with alpha heating turned off, shown in Fig. 11, indicate that both yield and normalized yield have a maximum at approximately the same Au thickness and lend credence to the notion that indeed, some Au is better than none. The main point is that the yield is even higher for this perturbation than for the initial scan with Be thickness. In other words, the 1D analysis validates that there exists a double-shell design what could lead to ignition – the point of this white paper. It remains for designers with 2D and 3D codes to go further with design optimization. The supposition is that double shells on Z could provide a robust fusion platform for research in future topics of interest. Additionally, it provides a new platform, completing the set of laser/magnetic direct and indirect-drive venues, and it complements hohlraum experiments scheduled for fusion research on NIF.

This new, magnetically-driven indirect drive with double shells has unverified potential but untapped opportunity. Hammer writes in the second sentence of Ref. 6 that "the important milestone of alpha particle heating – doubling the yield due to self-heating – appears likely to be within reach". Indeed, Hurricane[16] shows this with recent NIF data. The point to take home is that with alpha heating turned on, Helios shows a double-shell design that increases fusion yield not a factor two but by nearly 90X with a uniform 220-eV radiation drive. Hammer's paper[6] already addresses for a single shell how

ignition could be accomplished on a Z machine upgraded to 16 MJ pinch energy. A double shell might be easier. We have demonstrated in this paper that a 10% increase in capsule radius resulted in more than a one-hundred fold increase in neutron yield. Depending on how big a hohlraum can be filled with symmetric drive, one could imagine a several-mm radius capsule with all the yield one could want.

Conclusion: To summarize the main point, there exist two unique Z platforms studied in the past, either of which may serve to provide the necessary double-sided hohlraum drive to reach fusion ignition, but neither of which has been characterized in detail. We find through this study that in 1D implosions a double-shell capsule design using these platforms could be very interesting on Z today, and even more so if we build a larger pulsed power facility than Z in the future. We note that since the primary z-pinch x-ray sources are outside of the secondary capsule-containing hohlraum, these platforms could potentially complement laser-driven hohlraum experiments on the NIF and provide clues to how the different drives affect the capsule physics.

We close with issues in the text to be resolved and some problems that were not considered:

- Symmetry within the secondary hohlraum and time-dependent Legendre modes,
- Sufficient T_{rad} over sufficient volume – hohlraum size,
- Absence of preheat for the various possible drives (addressed briefly in the appendix),
- Target fabrication (not a problem unique to Z),
- Diagnostic access, and
- Determination of how much relaxation of drive current and energy needs derives from double-shell capsules; i.e., is the present capability sufficient?

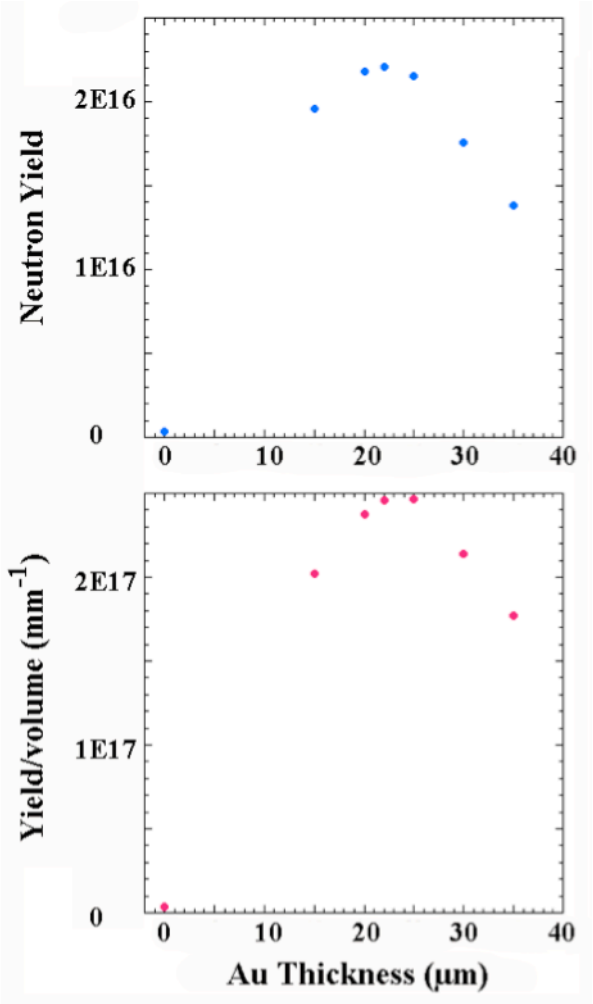

Figure 11. Dependence of yield (top) and yield/volume of DT (bottom) on the thickness of the inner Au shell

These factors would figure early on into a program to explore the capabilities of a successful ignition campaign at Sandia. We advocate that more detailed 2D/3D studies be conducted to motivate this fourth fusion approach.

References

1. G A Rochau, J E Bailey, G A Chandler, G Cooper, G S Dunham, P W Lake, R J Leeper, R W Lemke, T A Mehlhorn, A Nikroo, K J Peterson, C L Ruiz, D G Schroen, S A Slutz1, D Steinman, W A Stygar and W Varnum, Plasma Phys. Control. Fusion **49** B591 (2007).

2. T. W. L. Sanford, T. J. Nash, and R. C. Mock, D. L. Peterson, R. G. Watt, and R. E. Chrien, J. P. Apruzese and R. W. Clark, N. F. Roderick,G. S. Sarkisov, M. G. Haines, Phys. Plasmas **12**, 22701 (2005)

3. R. E. Olson, G. A. Chandler, M. S. Derzon, D. E. Hebron, J. S. Laser, R. J. Leeper, T. J. Nash, G. E. Rochau. T. W. L. Sanford, N. B. Alexander, C. R. Gibson, Fusion Tech. **35**, 261 (1999).

4. R. A. Vesey, M. C. Herrmann, R. W. Lemke, M. P. Desjarlais, M. E. Cuneo, W. A. Stygar, G. R. Bennett, R. B. Campbell, P. J. Christenson, T. A. Mehlhorn, J. L. Porter, and S. A. Slutz, Phys. Plasmas **14**, 056302 (2007).

5. J. A. Cobble, A. V. Bessarab, A. V. Kunin, V. A. Tokarev, S. R. Goldman, Plasma Physics Reports, **24**, 180 (1998).

6. J. Hammer, 8th Intern. Conf. Inertial Fusion Science and Appl. (IFSA 2013), J. Phys. Conf. Series **688**, 012025 (2016).

7. M. E. Cuneo, R. A. Vesey, G. R. Bennett, D. B. Sinars, W. A. Stygar, E. M. Waisman, J. L. Porter, P. K. Rambo, I. C. Smith, S. V. Lebedev, J. P. Chittenden, D. E. Bliss, T. J. Nash, G. A. Chandler, B. B. Afeyan, E. P. Yu, R. B. Campbell, R. G. Adams, D. L. Hanson, T. A. Mehlhorn, M. K. Matzen, Plasma Phys. Control. Fusion **48**, R1-R35 (2006).

8. J. A. Cobble, T. E. Tierney, N. M. Hoffman, B. G. DeVolder, D. C. Swift, Phys. Plasmas **13**, 056304 (2006). The reference does not make this point explicitly, but it was the experience of the first author, in analyzing Dante data, that this was the case.

9. G. A. Kyrala, A. Seifter, J. L. Kline, S. R. Goldman, S. H. Batha, N. M. Hoffman, Phys. Plasmas **18**, 072703 (2011).

10. T. A. Mehlhorn, J. E. Bailey, G. Bennett, G. A. Chandler, G. Cooper, M. E. Cuneo, I. Golovkin, D. L. Hansen, R. J. Leeper, J. J. MacFarlane, R. C. Mancini, M. K. Matzen, T. J. Nash, C. L. Olson, J. L. Porter, C. L. Ruiz, D. G. Schroen, S. A. Slutz, W. Varnum, R. A. Vesey, Plasma Phys. Control Fusion **45**, A435 (2003).

11. www.prism-cs.com/Software/Helios/Helios_documentation.htm

12. Bill Daughton, LANL, is the author of the version shown in Fig. 4. It has not been published, and it is an evolving design. It will be different for ZR drive because the drive history is different.

13. P. Amendt, J. D. Colvin, R. E. Tipton, D. E. Hinkel, M. J Edwards, O. L. Landen, J. D. Ramshaw, L. J. Suter, W. S. Varnum, R. G. Watt, Phys. Plasmas **9**, 2221 (2002).

14. G. A. Rochau *et al*., "High-Performance Capsule Implosion

Driven by the Z-pinch Dynamic Hohlraum", European Physical Society – Division of Plasma Physics, July 6, 2006

15. Chris Hamilton, MST-7, LANL, private communication.

16. O. A. Hurricane, D. A. Callahan, D. T. Casey, P. M. Celliers, C. Cerjan, E. L. Dewald, T. R. Dittrich, T. Döppner, D. E. Hinkel, L. F. Berzak Hopkins, J. L. Kline, S. Le Pape, T. Ma, A. G. MacPhee, J. L. Milovich, A. Pak, H.-S. Park, P. K. Patel, B. A. Remington, J. D. Salmonson, P. T. Springer & R. Tommasini, Nature **506**, 343 (2014).

A1. L. Yin, B. J. Albright, H. A. Rose, K. J. Bowers, B. Bergen, R. K. Kirkwood, D. E. Hinkel, A. B. Langdon, P. Michel, D. S. Montgomery, and J. L. Kline, Phys. Plasmas **19**, 056304 (2012).

A2. http://henke.lbl.gov/optical_constants/ (Au, 30 μm).

Appendix A: Preheat

Conventional wisdom is that radiation from W wire arrays could be accompanied with W L-band radiation at stagnation – well after a capsule would have imploded, but these lines have been observed in time-integrated spectra, as well as a continuum from 10 – 100 keV. Among the first experimental goals of an ICF campaign on Z would be to assess this phenomenon. By way of comparison, NIF has really suffered. Yin *et al*. report[A1] that consistent with 1-MJ experiments, theory predicts time-averaged SRS (stimulated Raman) backscatter values between 30% and 40% for the inner beam. About 10% of laser beam energy goes into non-thermal hot electrons with energy above 30 keV. The SRS hot-electron energy increases with increasing laser intensity (> 1-MJ shots). Electron preheat from LPI is not a problem Z hohlraums have to survive. At NIF, a second preheat source from hot electrons arises when they strike the hohlraum walls. "They excite x-ray emission which may contribute to capsule preheat."[A1] The preheat shields at NIF are designed to stop Au M-band radiation. But, 30-keV electrons can excite Au L band. The difference at Z is that such electrons are not born inside the hohlraum. For the double-ended wire-array DH, due diligence only requires that an inquiry be made. Unlike laser photons, multi-keV x rays do penetrate the surface of the hohlraum wall. Fluorescence emission first has to escape the wall to be harmful.

Finally, the double shell has an advantage over single-shell designs: the inner ~30-μm Au shell blocks[A2] >90% of x-ray preheat below ~25 keV. This is a huge advantage, another part that makes the double shell compelling. Clearly, however, a more sophisticated analysis is necessary.